

MULTI-OBJECTIVE OPTIMIZATION OF PARAMETERS AND LOCATION OF PASSIVE VIBRATION ISOLATION SYSTEM EXCITED BY CLAMPED THIN PLATE FOUNDATION

H. Wei^{1,3} - X. Jian² - Z. Da-Yong^{1,3*} - W. Ying-Lei^{1,3} - L. Jian-Wei⁴ - L. Kun-Lin^{1,3}

¹ School of Civil and Hydraulic Engineering, Hefei university of technology, Hefei, China

² China National Machinery Industry Corporation, Beijing, China

³ Anhui Provincial Laboratory of Civil Engineering and Materials, Hefei, China

⁴ School of Mechanical and Automotive Engineering, Hefei university of technology, Hefei, China

ARTICLE INFO

Article history:

Received: 29.08.2014.

Received in revised form: 06.11.2014.

Accepted: 11.11.2014.

Keywords:

Precision equipment

Vibration isolators

Thin plate

Clamped

Passive vibration isolation

Displacement transmissibility

Multi-peak system

Multi-objective particle swarm optimization

Abstract:

This paper reports a novel optimization strategy combined with artificial intelligence for parameters and location design of precision equipment and provides a broader view for traditional passive vibration isolation. It also considers "precision equipment-vibration isolators-thin plate foundation" as a composite passive vibration isolation system and the clamped thin plate. The vibration isolation system is considered as four-point support, and the displacement amplitude transmissibility from the thin plate to precision equipment is derived and based on the analysis of influencing factors of transmissibility; subsequently, multi-objective optimization of the composite system is performed. A novel swarm intelligence multi-objective optimization method—a multi-objective particle swarm optimization (MOPSO) algorithm is adopted in this paper which can achieve a global optimal solution and by selecting the desired solution from an equivalence relation, the whole Pareto set can be avoided. The maximum and variance of the four transmitted peak displacements are simultaneously considered as fitness functions, and the purpose is to reduce the amplitude of the multi-peak isolation system, and in the meantime, to allow the plate to be uniformly vibrated as far as possible. Moreover, the presented idea is validated numerically, and the location research of the precision equipment mounted on the plate is also conducted.

* Corresponding author. Tel.: +86 551 6291 9186
E-mail address: zhudymeng@163.com

1 Introduction

Precision equipments for engineering application include high-precision measuring, scanning equipment, etc.; advances in science and technology is gradually prompting these equipments to move fast towards the ultra-precision era. Since vibration is a key problem in the process of utilizing precision equipments, isolating and attenuating the harmful vibration from the surrounding environment to the equipments play a significant role.

Passive methods are commonly utilized for vibration isolation of sensitive equipments, and the performance is closely related to the parameters configuration; appropriate parameters can improve the isolation performance, otherwise, it will be counterproductive; therefore, it is very necessary to perform an optimal design of the isolation system. Rivin [1] conducted a systematic study of the precision isolation system affected by the environmental micro vibration, and several design principles involved in the isolation system were discussed. Veprík et al. [2] performed a study for the sophisticated electronic equipment excited by intense harmonic load, and optimal stiffness and damping were also studied. Ideal passive design of micro-vibration isolation of the sensitive platform in the spacecraft was performed by the optimal location placement of reaction wheel assemblies (RWA). Wu and Wang [3] investigated the feasibility of utilizing eigenvector assignment by enhancing vibration isolation performance of periodic isolators, and the eigenvectors of this integrated system were selected such that the modal energy in the concerned coordinates was minimized by using the Rayleigh Principle. An optical cavity was designed and implemented in the Ref. [4]. Since the cavity was insensitive to vibration in all directions, it was mounted with its optical axis in the horizontal plane. An experimental evaluation of the whole-spacecraft passive isolation system was presented with a demonstration unit consisting of a series of isolator elements inserted in the joints between the adapter and the launch vehicle [5]. In the Ref. [6], both the condensed model and the simplified model of the whole-spacecraft vibration isolation system were obtained based on Craig – Bampton component modal synthesis and the theory about modal effective mass. Traditional isolation design of engineering equipments is generally based on the assumption that the foundation is absolutely

rigid, and that the vibration participation is not considered. However, when the external stimulus is high-frequency, and the foundation stiffness is low, the vibration isolation cannot reach an ideal effect if traditional strategies are still being adopted, and if they even make the dynamic performance deteriorate. Therefore, in engineering practice, vibration participation of foundation must be taken into account. A thin plate model is a common foundation form of equipment vibration isolation, and in general, a thin plate is simply supported in view of calculation simplicity; however, clamped forms cannot be ignored for its wide range of applications, such as the floors of industrial buildings. Amabili et al. [7] performed a study of large-amplitude forced vibration of a clamped stainless steel plate excited by centralized harmonic force. Guofa et al. [8] carried out numerical simulation of cast steel plate, and two optimization schemes were completed based upon the simulation presented. Ref. [9] conducted a comparative study of active and passive vibration isolation of a clamped thin plate which was aimed at examining piezoelectric materials in active vibration control. Ref. [10] solved the free vibration problem of clamped thin plates by using quasi Green function. Arenas [11] derived the general numerical expression of clamped thin plate vibration with virtual work principle; and as it was not necessary to solve simultaneous equations, these solutions could be easily calculated and programmed; in the meantime, complex symmetric characteristics of the Rayleigh-Ritz method can be overcome here, and consequently, they can create favourable conditions for combining the equipments, isolators and thin plate foundation as a composite system.

In general, the traditional gradient-based optimization requires the computations of sensitivity factors and eigenvectors during its iterative process. This causes a heavy computational burden and slow convergence. Moreover, there is no local criterion for deciding whether a local solution is also the global solution. Thus, the conventional optimization methods using derivatives and gradients are generally not able to locate or identify the global optimum; however, for real-world applications, one is often content with a good solution, even if it is not the best solution. Consequently, heuristic methods are widely used for the global optimization problem. Particle swarm optimization (PSO) algorithm was first proposed by

Eberhart and Kennedy [12], and it is a novel population-based metaheuristic algorithm utilizing the swarm intelligence generated by the cooperation and competition between the particles in a swarm and emerging as a useful tool for engineering optimization.

Coello et al. [13] first proposed the multi-objective particle swarm optimization (MOPSO) algorithm, and the main idea is that by determining the flying direction of the particles with optimal Pareto sets and a set of non-dominated solutions found in global knowledge base data before, the particles flying in the search space can be guided, and a unique, optimal and global solution can be obtained by means of a specific algorithm. MOPSO can overcome the disadvantage of traditional multi-objective methods (such as SPEA and SPEA 2, etc.), e.g., the desired solution must be selected from a group of equivalent Pareto set [14].

2 Composite passive vibration isolation system

Passive vibration isolation system of typical precision equipment is shown in Fig. 1.

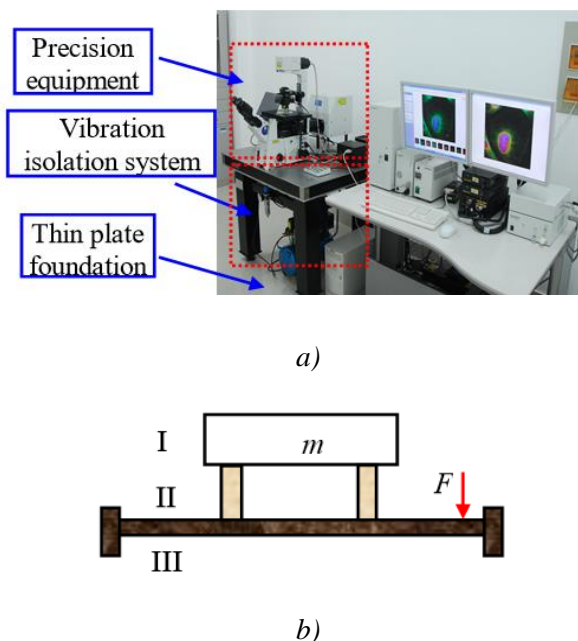


Figure 1. Composite passive vibration isolation system: a) Typical precision equipment b) Simplified vibration isolation model.

In Fig. 1 (b), I denotes the precision equipment, II denotes the isolators, including the stiffness and

damping components, and III denotes the clamped rectangular thin plate foundation. m is the mass of precision equipment which is supported by four isolators mounted on the thin plate, and stiffness and damping of each isolator can be denoted as $k_i, c_i (i = 1 \sim 4)$. The geometry of the plate is $a \times b \times h$, and the equipment can be simplified as a cuboid whose plane size is $e \times f$. The centralized harmonic excitation force on the plate is $F e^{j\omega t}$, F is the amplitude, and ω is the circular frequency. I, II, III are considered as a composite isolation system which can be expressed in Cartesian coordinates and shown in Fig. 2, O is the coordinate origin, A, B, C and D are the four corner installation locations of precision equipment.

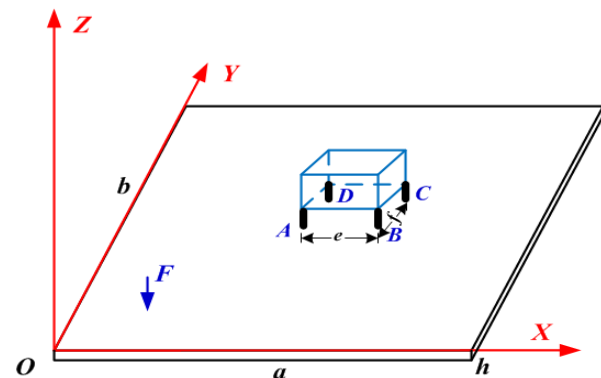


Figure 2. Schematic diagram of the vibration isolation system expressed in Cartesian coordinate system.

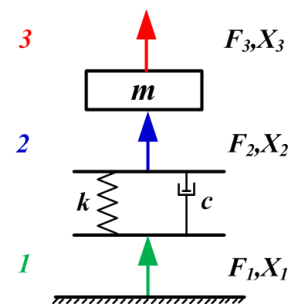


Figure 3. Schematic diagram of four-pole parameters of the vibration isolation system.

From Fig. 3, the following formula can be derived according to four-pole parameter connection characteristics:

$$\begin{bmatrix} F_1 \\ X_1 \end{bmatrix} = [k_{ij}^*][m_{ij}] \begin{bmatrix} F_3 \\ X_3 \end{bmatrix}, \quad (1)$$

where $[m_{ij}]$ is the four-pole parameter of mass, $[k_{ij}^*]$ is the four-pole parameter of the stiffness and damping in parallel, and

$$[k_{ij}^*] = \begin{bmatrix} 1 & 0 \\ \frac{1}{k+ic\omega} & 1 \end{bmatrix}, [m_{ij}] = \begin{bmatrix} 1 & -m\omega^2 \\ 0 & 1 \end{bmatrix}. \quad (2)$$

The following equations can be derived by transforming Eq. (1):

$$\begin{bmatrix} F_1 \\ X_1 \end{bmatrix} = \begin{bmatrix} \Omega_{11} & \Omega_{12} \\ \Omega_{21} & \Omega_{22} \end{bmatrix} \begin{bmatrix} F_3 \\ X_3 \end{bmatrix} = \begin{bmatrix} 1 & -m\omega^2 \\ \frac{1}{k+ic\omega} & 1 - \frac{m\omega^2}{k+jc\omega} \end{bmatrix} \begin{bmatrix} F_3 \\ X_3 \end{bmatrix}, \quad (3)$$

$$X_1 = \Omega_{21}F_3 + \Omega_{22}X_3. \quad (4)$$

Suppose $F_3/X_3=Z_m$, Z_m denotes the mechanical impedance of the presented equipment, and then divide the both sides of Eq. (4) by X_3 :

$$\frac{X_1}{X_3} = \frac{1}{\Omega_{21}Z_m + \Omega_{22}}. \quad (5)$$

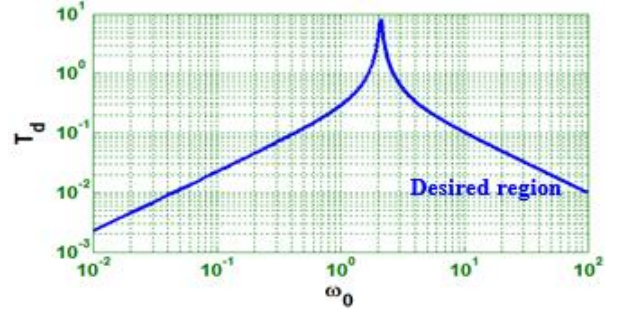
Thus the displacement transmissibility can be derived as:

$$T_d = \left| \frac{X_3}{X_1} \right| = \frac{\sqrt{k^2 + c^2\omega^2}}{\sqrt{(Z_m + k - m\omega^2)^2 + c^2\omega^2}}. \quad (6)$$

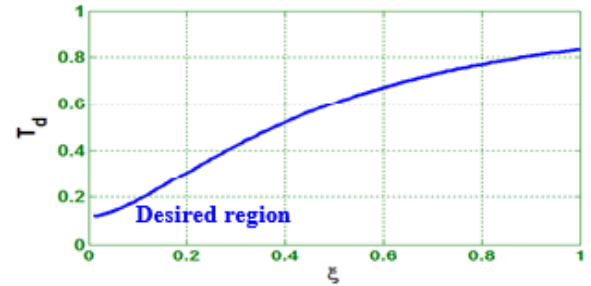
Introduce the parameters $\omega_0 = \sqrt{k/m}$, $\zeta = c/(2m\omega_0)$, $E = Z_m/m$, thus Eq. (7) can be converted into:

$$T_d = \sqrt{\frac{\omega_0^4 + (2\zeta\omega\omega_0)^2}{(E + \omega_0^2 - \omega^2)^2 + (2\zeta\omega\omega_0)^2}}. \quad (7)$$

Seen from Eq. (7), T_d is a complex function as the variables of ω_0 , ω , m , ζ , Z_m ; in specific working condition, ω , m , Z_m ; can be regarded as constants, thus T_d can be simply referred to as $\Gamma(\omega_0, \zeta)$, and variation curves of the remaining undetermined parameters are depicted in Fig. 4.



a) $T_d - \omega_0$



b) $T_d - \zeta$

Figure 4. Variation curves of the T_d .

Seen from the Fig. 4, in the desired region, T_d decreases when ω_0 is increased, yet it will increase when ζ_0 is increased.

3 Numerical simulation of the clamped thin plate vibration

Based on the virtual work principle, Arenas derived the general form of displacement solutions of the clamped thin plate excited by centralized harmonic force as following:

$$X(x,y) = F \sum_{m=1}^{\infty} \sum_{n=1}^{\infty} \frac{\Psi_{nm}(x,y)\Psi(x',y')}{B(I_1 I_2 + 2I_3 I_4 + I_5 I_6) - \rho_s \omega^2 I_2 I_6}, \quad (8)$$

$B = Eh^3/[12(1-\nu^2)]$ is the bending stiffness of the thin plate; E is the Young's modulus; ν is the Poisson's ratio; $\rho_s = \rho h$ is the surface density of the thin plate, and ρ is the volume density; (x,y) is a random discrete point on the plate, and (x',y') is the position of the external dynamic force.

In practice, the infinite series expansion of Eq. (8) are often truncated into a finite term, and in this paper, $m, n = 1, 2, \dots, 6$.

Modal function $\psi_{nm}(x,y)$ is denoted as:

$$\Psi_{mn}(x,y) = \theta_m(x)\xi_n(y);$$

$$\theta_m(x) = J\left(\frac{\beta_m x}{a}\right) - \frac{J(\beta_m)}{H(\beta_m)} H\left(\frac{\beta_m x}{a}\right),$$

$$\xi_n(y) = J\left(\frac{\beta_n y}{b}\right) - \frac{J(\beta_n)}{H(\beta_n)} H\left(\frac{\beta_n y}{b}\right), \quad (9)$$

$J(\bullet) = \cosh(\bullet) - \cos(\bullet)$, $H(\bullet) = \sinh(\bullet) - \sin(\bullet)$, and β_i is the root of the formula $\cosh(\beta) \cos(\beta) = 1$;

$$I_2 I_6 = \frac{ab}{\beta_m \beta_n} L_m L_n; \quad I_3 I_4 = \frac{\beta_m \beta_n}{ab} R_m R_n;$$

$$I_1 = I_6 \left(\frac{\beta_m}{a}\right)^4; \quad I_5 = I_2 \left(\frac{\beta_n}{b}\right)^4;$$

$$L_i = \frac{(1 + D_i^2) \sinh(2\beta_i)}{4} + \sinh(\beta_i) [2D_i \sin(\beta_i) - (1 - D_i^2) \cos(\beta_i)]$$

$$- (1 + D_i^2) \sin(\beta_i) \cosh(\beta_i) + (1 - D_i^2) \sin(\beta_i) \cos(\beta_i) + \beta_i$$

$$- \frac{D_i [1 + \cosh(2\beta_i)]}{2} + D_i \cos^2(\beta_i);$$

$$R_i = \frac{(1 + D_i^2) \sinh(2\beta_i)}{4} - \frac{D_i \cosh(2\beta_i)}{2} - \frac{(1 - D_i^2) \sin(\beta_i) \cos(\beta_i)}{2}$$

$$- D_i \cos^2(\beta_i) - D_i^2 \beta_i + \frac{3D_i}{2}; \quad D_i = \frac{J(\beta_i)}{H(\beta_i)}. \quad (10)$$

For the purpose of visually presenting the vibration of the thin plate, a case is numerically studied to pave the way for further research.

3.1 Numerical example 1

The basic parameters of the plate are set as: $a = 3.0 \text{ m}$, $b = 6.0 \text{ m}$, $h = 0.2 \text{ m}$, $\rho = 7800 \text{ kg/m}^3$, $\nu = 0.33$, $E = 2.1 \times 10^{11} \text{ Pa}$; the force amplitude is $F = 10 \text{ N}$, and the coordinate of the exciting force is $(0.5454 \text{ m}, 0.9765 \text{ m})$. Discretize the thin plate so as to obtain the coordinate of any point (x,y) on the plate, and the accuracy settings are denoted as Δx , Δy , respectively.

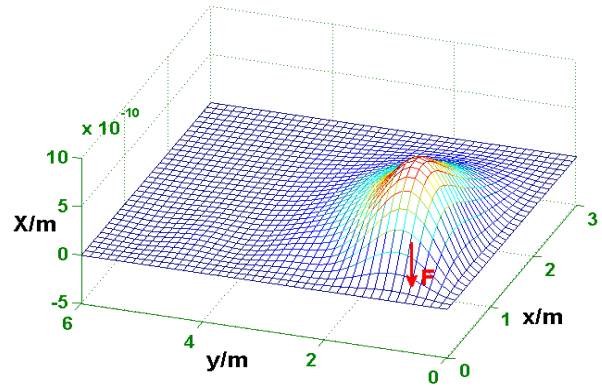
$$\Delta x = \text{linspace}(0, a, 34),$$

$$\Delta y = \text{linspace}(0, b, \text{round}(b/a \times 22)),$$

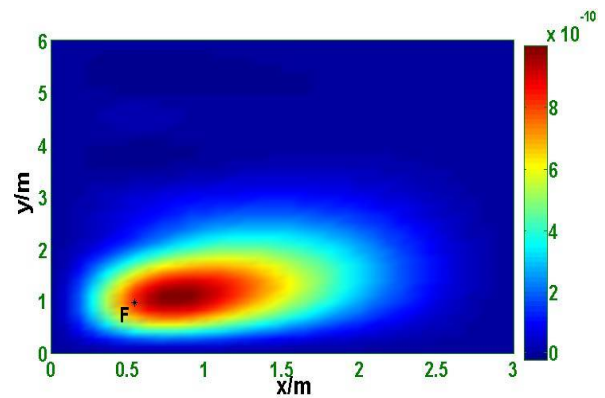
(*linspace* (-), *round* (-)) are respectively the operations based on MATLAB2010).

Vibration of the thin plate is schematically shown in Fig. 5; and with regard to the proposed principal

vibration modes of the thin plate, the dimensionless frequencies can be derived according to Ref. [11], which are listed in Table 1.



a) Plate vibration with discrete grid



(b) Plate vibration with pseudo-color contour

Figure 5. Schematic diagram of the thin plate vibration.

Table 1. Dimensionless frequency of principal modes for the clamped plate

$m \backslash n$	1 st	2 nd	3 rd	4 th	5 th	6 th
1 st	25	64	124	203	301	421
2 nd	32	71	131	210	309	431
3 rd	45	84	143	222	321	446
4 th	64	101	160	239	338	468
5 th	88	124	182	261	360	495
6 th	120	161	223	305	406	553

4 Brief introductions to MOPSO

In PSO algorithm, an own state of every particle can be described by a group of position and velocity vectors which represent the possible solutions and movement directions in the searching space, respectively. By constantly learning the found global and optimal solutions and the moving directions, and also by updating the neighbor optimal solutions, the desired solution can be obtained. The main steps of MOPSO are summarized as following:

Step 1: Initialize the population, and compute the corresponding objective function vectors of particles, and add the non-inferior solutions to the external archive;

Step 2: Initialize the local optimum $pbest$ of particles and the global optimum $gbest$;

Step 3: Amend the velocities and positions of the particles by evaluating the following equations so as to generate new $pbest$:

$$v_{ij} = \omega v_{ij}(t) + c_1 r_1 (pbest_{ij}(t) - x_{ij}(t)) + c_2 r_2 (gbest_{ij}(t) - x_{ij}(t)), \quad (11)$$

$$x_{ij}(t+1) = x_{ij}(t) + v_{ij}(t+1), \quad (12)$$

where i represents the i th particle; j represents the j th dimension of each particle; t represents the t th generation; $v_{ij}(t)$ represents the flight velocity vector; $x_{ij}(t)$ represents the flight displacement vector; $pbest$ represents the optimal location component; $gbest$ represents the optimal position of the entire particle swarm; c_1 , c_2 are acceleration factors or learning factors; and r_1 , r_2 are random numbers between $(0, 1)$. ω is the inertia weight factor which plays a key role in the PSO.

Step 4: Maintain the external archive with the obtained new non-inferior solution, and select $gbest$ for every particle (the archive determines the selection of the global optimum);

Step 5: Whether the maximum iteration is reached, or no, the program will continue; if yes, terminate the computation, and output the optimal *Pareto* solution set and the $gbest$. It is important to point out that, direct computation will generate a set of

equivalent solution when traditional multi-objective optimization is performed, and it is difficult to determine which the desired one is. Pareto dominating is the most direct way to solve this problem, namely, consider all of the non-inferior solutions in the archive, and determine a ‘leader’, and density measuring technique is commonly used to determine the global optimum. The nearest neighbor density estimation method [15] based on the nearest neighbor congestion evaluation of particles is adopted in this paper; certainly, there are also other similar methods, such as kernel density estimation method [16], etc.

5 Parameters and location optimization of the composite system using MOPSO

In traditional studies, the isolated objects are often simplified as a mass dot; however, the size of the equipment in practice cannot be ignored with respect to the foundation. As shown in Fig. 2, transmitted vibration from thin plate to precision equipment will bring about four different amplitudes which are extremely unfavorable for the normal use and maintenance of the equipments. Therefore, vibration of the sensitive equipment must be reduced as far as possible, meanwhile, the different vibrations should be more uniform through optimal design of parameters and installation location, thus both of the two objectives should be optimized simultaneously.

In Fig. 2, the original displacements of A, B, C, and D of the thin plate can be donated as X_A , X_B , X_C and X_D , respectively, and the transmitted displacement to the equipment can be respectively denoted as, $X_{mA} = |T_{dA}| X_A$, $X_{mB} = |T_{dB}| X_B$, $X_{mC} = |T_{dC}| X_C$ and $X_{mD} = |T_{dD}| X_D$ by means of the transmission principle described in Section 2.

The two fitness functions can be written as:

$$\begin{cases} fitness_1 = \max(|X_{mA}, X_{mB}, X_{mC}, X_{mD}|) \\ fitness_2 = var(X_{mA}, X_{mB}, X_{mC}, X_{mD}), \end{cases} \quad (13)$$

where $\max(\cdot)$ and $var(\cdot)$ are the maximum and variance operation based on MATLAB 2010. Fig. 6 shows the discrete grid of the thin plate and the installation location of precision equipment.

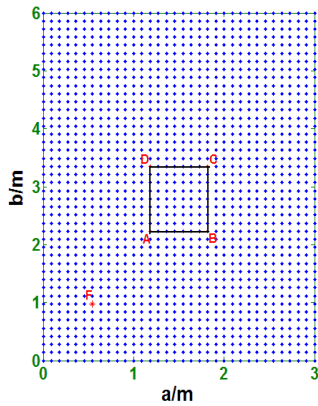


Figure 6. Discrete grid of the thin plate.

The basic idea of the multi-objective optimization can be organized in the following chart.

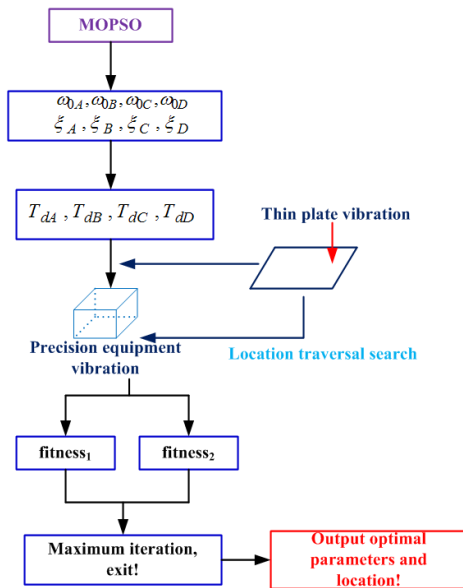


Figure 7. Idea chart of the multi-objective optimization.

5.1 Numerical example 2

Consider thin plate foundation described in section 3.1, equipment mass is supposed to be $m = 50$ kg, mechanical impedance $Z_m = 2000 \Omega$, and plane size of the thin plate is $e \times f = 0.71 \times 1.1$ m; the circular frequency of the external force is $\omega = 2\pi$ (rad/s). For the four isolators installed at A, B, C, and D, the natural frequencies and damping ratios can be denoted as $\omega_{0A}, \omega_{0B}, \omega_{0C}, \omega_{0D}, \zeta_A, \zeta_B, \zeta_C, \zeta_D$, respectively.

In MOPSO algorithm, the dimension is set as 8, namely:

$$swarm(i) = \omega_{0A} \sim \omega_{0B}, i = 1 \sim 4 \text{ and}$$

$$swarm(i) = \zeta_A \sim \zeta_B, i = 5 \sim 8;$$

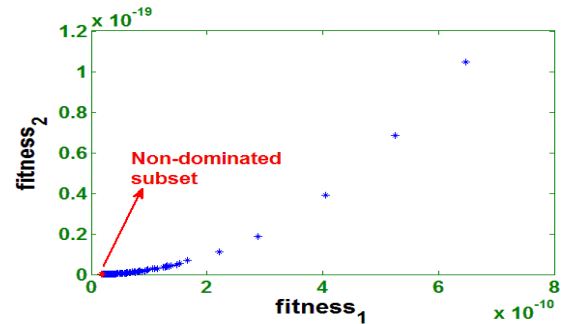
the searching scope is arbitrarily set as $[0.01, 0.01, 0.01, 0.01, 0.01, 0.01, 0.01, 0.01] \sim [100, 100, 100, 100, 1, 1, 1, 1]$ the population size is 200; the maximum iteration is 100; the learning factors are defined as $c_1 = 1.5, c_2 = 1.5$; linear changing strategy is used for the inertia weight factor ω [17], and $\omega_{max} = 0.9, \omega_{min} = 0.4$.

The equipment presented is non-equilateral in purpose of simulating the general case, and the following two location conditions should be involved in:

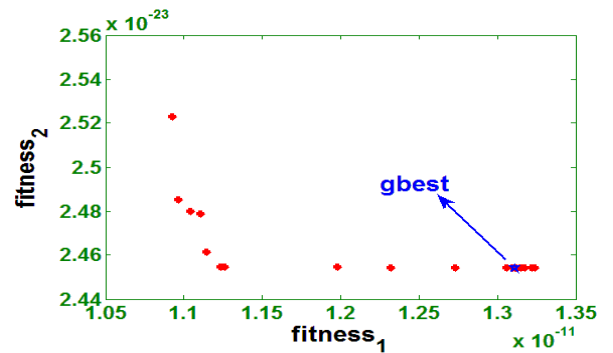
Case 1, the short size e of equipment is in parallel with the short size a of the plate;

Case 2, the short size e of equipment is in parallel with the long size b of the plate.

The optimization results of the two cases presented are listed in Fig. 8 and Fig. 9.



a) Non-dominated subset in the entire set



b) Gbest solution in the Pareto frontier

Figure 8. Multi objective optimization results (Case 1).

The *gbest* solution of Case 1 is 77.1334, 99.2055, 100, 99.5671, 0.01269, 0.01656, 0.01, 0.01044; thus the stiffness of the four isolators can be derived as $k_A = 2.9747 \times 10^5 \text{ N/m}$, $k_B = 4.9208 \times 10^5 \text{ N/m}$, $k_C = 5 \times 10^5 \text{ N/m}$, $k_D = 4.9568 \times 10^5 \text{ N/m}$, and the damping of the four isolators are respectively as $c_A = 97.8999 \text{ Ns/m}$, $c_B = 164.3198 \text{ Ns/m}$, $c_C = 100 \text{ Ns/m}$, $c_D = 104.3585 \text{ Ns/m}$.

After isolation, the peak displacements of A, B, C, and D of precision equipment are respectively as $X_{A, \max} = 1.3109 \times 10^{-11} \text{ m}$, $X_{B, \max} = 5.9761 \times 10^{-12} \text{ m}$, $X_{C, \max} = 3.3903 \times 10^{-12} \text{ m}$, $X_{D, \max} = 2.5499 \times 10^{-12} \text{ m}$; and the variance of the peak vector is 2.2999×10^{-23} . Optimal location of the precision equipment is obtained simultaneously by traversal searching, and the coordinate is A (0.8181 m, 1.1160 m), B (1.5281 m, 1.1160 m), C (1.5281 m, 2.2160 m), D (0.8181 m, 2.2160 m).

0.0262, thus the stiffness and damping of the four isolators are defined as $k_A = 2.9799 \times 10^5 \text{ N/m}$, $k_B = 4.7211 \times 10^5 \text{ N/m}$, $k_C = 3.9892 \times 10^5 \text{ N/m}$, $k_D = 4.2343 \times 10^5 \text{ N/m}$, $c_A = 161.8852 \text{ Ns/m}$, $c_B = 97.1717 \text{ Ns/m}$, $c_C = 202.1366 \text{ Ns/m}$, and $c_D = 241.2946 \text{ Ns/m}$, respectively.

Likewise, peak displacements of the four different locations of the equipment are defined as:

$$X_{A, \max} = 1.3376 \times 10^{-11} \text{ m}, X_{B, \max} = 3.5591 \times 10^{-12} \text{ m}, X_{C, \max} = 3.9693 \times 10^{-12} \text{ m}, X_{D, \max} = 5.9951 \times 10^{-12} \text{ m};$$

and the variance is 2.0796×10^{-23} . Similarly, the coordinate of the optimal installation location is: A (0.8181 m, 1.1160 m), B (1.9181 m, 1.1160 m), C (1.9181 m, 1.8260 m), D (0.8181 m, 1.8260 m).

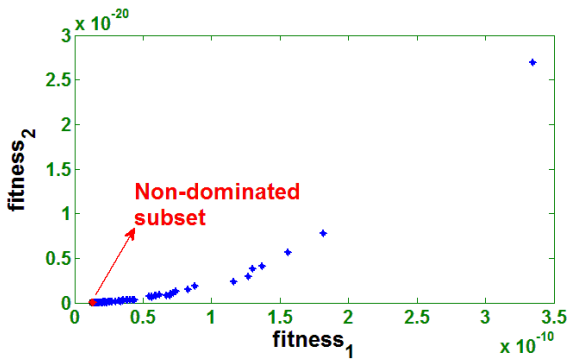
Seen from the optimization results, the maximum of the four peak displacements of Case 1 is a little lower than Case 2, but the variance of the former is higher than the latter; overall, the two cases for location placing are nearly equal in practice.

In theoretical perspective, finer mesh of the thin plate can lead to more reasonable location of the precision equipment; however, a moderate accuracy of a discrete grid is adopted in this paper in view of computation efficiency. In addition, arbitrary installation style can be considered when the plate is of unlimited fine mesh, namely, the equipment needs not be in parallel with the plate foundation; but it is quite uneasy to perform this method with general mesh accuracy, because making the searched locations of the plate match the size of the equipment well is a little difficult and the generated error may be large, and this strategy is not adopted here.

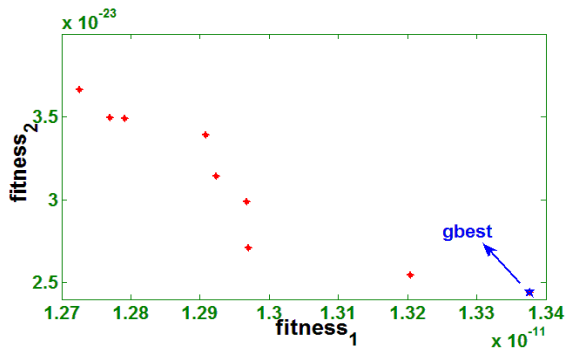
It is also worth mentioning that, the isolated equipment is considered as four-point support here, but the optimization idea will be completely equal to other supporting methods (such as six-point, eight-point, etc).

6 Conclusions

In this paper, theoretical research of clamped plate vibration is combined with isolation system of precision equipment, and a novel composite system is proposed which is aimed at simulating the micro vibration of sensitive equipments excited by



a) Non-dominated subset in the entire set



b) Gbest solution in the Pareto frontier

Figure 9. Multi-objective optimization results (Case 2).

For this case, the *gbest* is 77.1998, 97.1717, 89.3224, 92.0256, 0.0209, 0.0100, 0.0226,

surrounding environment. Novel multi-objective optimization method—MOPSO is adopted here, and the unique *gbest* can be obtained; much lower amplitude and more uniform vibration of the multi-peak system are defined as the isolation objects, and this idea is validated numerically.

This study provides a broader idea for engineering equipment isolation, and it also has certain significance in practical design of industrial manufacturing. Meanwhile, it is also aimed at preparing the revising work of national code of China—"Code for design of vibration isolation".

Acknowledgments

This research was completely supported by National Natural Science Foundation of China, and the Grant Nos. are 51078123, 51179043. Valuable comments and suggestions by preparation experts of the national code—"Code for vibration load design of industrial building" on the ideas carried out are gratefully acknowledged.

References

- [1] Rivin, E. I.: *Vibration isolation of precision equipment*, Precision Engineering, 17 (1995), 1, pp. 41-56.
- [2] Veprik, A. M., Babitsky, V. I.: *Vibration protection of sensitive electronic equipment from harsh harmonic vibration*, Journal of sound and vibration, 238 (2000), 1, pp. 19-30.
- [3] Wu, T. Y., Wang, K. W.: *Periodic isolator design enhancement via vibration confinement through eigenvector assignment and piezoelectric circuitry*, Journal of Vibration and Control, 13 (2007), 7, pp. 989-1006.
- [4] Webster, S. A., Oxborrow, M., Gill, P.: *Vibration insensitive optical cavity*, Physical Review A, 75 (2007), 1, 011801.
- [5] Jun, Z., Hong, X. H., Zhi, Y. Z.: *An evaluation of the whole-spacecraft passive vibration isolation system*, Proceedings of the Institution of Mechanical Engineers, Part G: Journal of Aerospace Engineering, 221 (2007), 1, pp. 67-72.
- [6] Liu, L. K., Zheng, G. T.: *Parameter analysis of PAF for whole-spacecraft vibration isolation*, Aerospace science and technology, 11 (2007), 6, pp. 464-472.
- [7] Amabili, M., Carra, S.: *Experiments and simulations for large amplitude vibrations of rectangular plates carrying concentrated masses*, Journal of Sound and Vibration, 331 (2012), 1, pp. 155-166.
- [8] M. Guofa, L. Changyun, G. Zeng: *Application of numerical simulation on cast steel toothed plate*, Engineering Review, 34 (2014), 1, pp. 1-6.
- [9] Kozupa, M. M., Wiciak, J. W.: *Comparison of passive and active methods for minimization of sound radiation by vibrating clamped plate*, Acta Physica Polonica, A., 119 (2011), pp. 1013-1017.
- [10] Li, S., Yuan, H.: *Green quasifunction method for free vibration of clamped thin plates*, Acta Mechanica Solida Sinica, 25 (2012), 1, pp. 37-45.
- [11] Arenas, J. P.: *On the vibration analysis of rectangular clamped plates using the virtual work principle*, Journal of Sound and Vibration, 266 (2003), 4, pp. 912-918.
- [12] Eberhart, R. C., Kennedy, J.: *A new optimizer using particle swarm theory*, Proceedings of the sixth international symposium on micro machine and human science, Nagoya, 1995, pp. 39-42.
- [13] Coello, C. A., Lechuga, M. S.: *MOPSO: A proposal for multiple objective particle swarm optimization*, Proceedings of the 2002 Congress on IEEE, Honolulu, 2002, pp. 1051-1056.
- [14] Fonseca, C. M., Fleming, P. J.: *An Overview of Evolutionary Algorithms in Multi-objective Optimization*, Evolutionary Computation, 3 (1995), 1, pp. 1-16.
- [15] Deb, K., Pratap, A., Agarwal, S., et al: *A fast and elitist multi-objective genetic algorithm: NSGA-II*, Evolutionary Computation, IEEE Transactions on, 6(2002), 2, pp. 182-197.
- [16] Goldberg, D. E., Richardson, J.: *Genetic algorithms with sharing for multimodal function optimization*, Genetic algorithms and their applications: Proceedings of the Second International Conference on Genetic Algorithms, Massachusetts, 1987, pp. 41-49.
- [17] Shi, Y., Eberhart, R.: *A modified particle swarm optimizer*, IEEE World Congress on Computational Intelligence, Anchorage, 1998, pp. 69-73.